Tome 22 N° 10 OCTOBRE 1987

REVUE DE PHYSIQUE APPLIQUÉE

Revue Phys. Appl. **22** (1987) 1131-1138 OCTOBRE **1987,** PAGE 1131

Classification
Physics Abstracts
61.12 — 68.65 — 71.70 — 75.25 — 75.80

Crystal and magnetic structures of $Fe_{0.25}TiSe_2$ and $Fe_{0.48}TiSe_2$

G. Calvarin ([1]), J. R. Gavarri ([1]), M. A. Buhannic ([2]), P. Colombet ([2]) and M. Danot ([2])

([1]) L.C.P.S., U.A. CNRS n° 453, Ecole Centrale, Grande Voie des Vignes, 92290 Châtenay-Malabry, France
([2]) Laboratoire de Chimie des Solides, U.A. CNRS n° 279, 2, rue de la Houssinière, 44072 Nantes Cedex 03, France

(*Reçu le 16 février 1987, révisé le 21 mai 1987, accepté le 26 juin 1987*)

Résumé. — Les structures cristallographiques et magnétiques des composés lamellaires antiferromagnétiques Fe_xTiSe_2 (x = 0,25 et 0,48) ont été déterminées à partir de l'affinement des spectres de diffraction de neutrons réalisés sur poudres dans le domaine 2-300 K. Une permutation partielle entre les sous-réseaux du fer et du titane est mise en évidence. Pour les deux composés, elle correspond à une substitution de 8 % du fer par le titane. La distorsion de l'octaèdre $TiSe_6$ s'atténue de x = 0,25 à x = 0,48, à savoir lorsqu'augmente le remplissage de la sous-bande d par suite du transfert de charge consécutif à l'intercalation. Pour la phase $Fe_{0,48}TiSe_2$ magnétiquement ordonnée, l'arrangement des spins permet d'expliquer l'effet magnéto-élastique précédemment observé. L'origine du phénomène réside dans la nature ferromagnétique de l'interaction entre premiers voisins fer le long de **b** ($d_{Fe\text{-}Fe}$ = 3,59 Å), dont l'intensité augmente lorsqu'ils se rapprochent. Les spins des électrons de conduction du titane sont notablement polarisés par les moments localisés du fer, ce qui se traduit par l'établissement au-dessous de T_N d'une onde de densité de spin commensurable. L'affinement des intensités des spectres à 2 K conduit à l'attribution d'un moment de 0,07(3) et 0,31(3) μ_B pour x = 0,25 et x = 0,48 respectivement.

Abstract. — The crystal and magnetic structures of the lamellar Fe_xTiSe_2 (x = 0.25 and 0.48) antiferromagnets have been refined from neutron diffraction powder data at several temperatures ranging from 2 to 300 K. For both compounds, Ti is found to be substituted for 8 % of Fe so that the separation of the two metals is not complete. The distortion of the Ti-containing octahedra decreases from x = 0.25 to x = 0.48 i.e. as the lower-occupied d-subband filling increases due to charge transfer upon intercalation. The origin of the previously evidenced magneto-elastic effect for x = 0.48 is shown to lie in the existence of ferromagnetic coupling between nearest-neighbouring iron moments along **b** ($d_{Fe\text{-}Fe}$ = 3.59 Å), the exchange parameter of which increases with decreasing distance. The Ti conduction electron spins are shown to be greatly polarized by the Fe localized moments leading to the onset of a commensurate spin density wave below T_N. The refinement of the 2 K intensities yields Ti moment values equal to 0.07(3) and 0.31(3) μ_B for x = 0.25 and 0.48, respectively.

1. Introduction.

The M_xTX_2 compounds (M and T are transition metal elements, X is S or Se) have been the subject of numerous investigations in the field of intercalation chemistry and physics [1], the layered dichalcogenide TX_2 being the host and M the intercalant. For T = Ti, the Fe, Co and Ni guests have been shown [2] to partially occupy the octahedral interstices in the van der Waals gap of the CdI_2-type host structure (hexagonal cell parameters : a' and c'). Arnaud *et al.* [2], have reported an extensive structural work devoted to the Fe_xTiSe_2 compounds. They have shown that for $x > 0.20$ superstructures occur due to an ordering of iron and vacancies. $Fe_{0.25}TiSe_2$ belongs to the M_5X_8 structural type ($FeTi_4Se_8 = M_5X_8$) whereas $Fe_{0.50}TiSe_2$ belongs to the Cr_3S_4 one ($FeTi_2Se_4 = M_3X_4$) as both defined by Chevreton [3]. They are described according to monoclinic cells, with constants and space group as follows :

$$a = 2a'\sqrt{3}\,;\quad b = 2a'\,;\quad c = 2c'\,;\qquad F2/m\ (x = 0.25)\,,$$

$$a = a'\sqrt{3}\,;\quad b = a'\,;\quad c = 2c'\,;\qquad I2/m\ (x = 0.50)\,.$$

The non conventional face-centred cell was used

because of its direct relationship to the hexagonal pseudo-cell.

From the viewpoint of the magnetic properties, the behaviour of the M_xTiSe_2 compounds strongly depends not only on the nature of M, but also on its amount. Magnetic properties of Fe_xTiSe_2 ($0 < x < 0.50$) powder samples were recently reexamined in detail [4]. For $x < 0.20$, the Fe-vacancy distribution is disordered and a spin-glass behaviour is observed at lower temperatures. In contrast, for $x > 0.20$, antiferromagnetic (AF) ordering takes place, in agreement with the above discussed superstructures occurrence, thus confirming the work by Muranaka and Takada [5]. The oxidation state of Fe is unambiguously equal to two.

In a previous study [6], the crystallographically ordered Fe_xTiSe_2 ($x = 0.25$, 0.38 and 0.50) compounds have been investigated as a function of temperature using susceptibility (χ) measurements, Mössbauer spectroscopy, and X-ray diffraction. As T decreases below T_N, χ parallel to the layers is constant whereas χ perpendicular to the layers decreases. Thus, the easy axis is perpendicular to the layers. From the evolution of the isomer-shift of Fe(II) against x, it was found that the coupling between the iron-*d* localized and the $TiSe_2$-band levels decreases as x increases, contrary to what is observed for lower iron contents in the disordered materials. For $x = 0.50$, magnetostriction was evidenced at T_N : the c parameter, the direction of which is close to that of the easy axis, expands, whereas the b parameter contracts. Besides, the consequences of iron intercalation in $TiSe_2$ were analysed as far as the crystal dimensionality, as deduced from the thermal expansion study, is concerned.

However, the exact crystal structure of these ordered AF materials remained to be determined. In particular, the question of a disorder induced by slight departures from stoichiometry [7] and that of an intricate Fe-Ti exchange [2] were not solved. The reasons of the lack of data in this area are (i) Fe and Ti are quasi indistinguishable using X-ray diffraction techniques, and (ii) no good crystal can be obtained due to twinning. Furthermore, the magnetic structures were unknown.

Consequently, as the coherent neutron scattering lengths of Fe and Ti are significantly different, we have undertaken the analysis of the neutron diffraction patterns of polycrystalline Fe_xTiSe_2 ($x = 0.25$ and 0.50) from 2 to 300 K. The goals of the present work are to solve, respective to the iron amount, (i) the crystal structure, in particular the question of the possible Fe-Ti substitution, (ii) the consequences of antiferromagnetic ordering as far as the Fe-site dimensions are concerned, and finally (iii) the low-temperature magnetic structure. In particular, the origin of magnetostriction for $x = 0.50$ has been supposed [6] to be the lowering of the spin system energy which results from the contraction of b due to the related increase of the exchange integral of the nearest-neighbour interaction along this direction. Following the Goodenough-Kanamori rules, the direct $t_{2g} - t_{2g}$ Fe(II) exchange is ferromagnetic (F) so that we have predicted a F alignment of the spins along the b-direction. This assumption required to be confirmed.

2. Experimental.

Polycrystalline Fe_xTiSe_2 ($x = 0.25$ and 0.50) were synthesized following the procedure given elsewhere [2]. Neutron diffraction patterns were recorded on the D1A diffractometer ($\lambda = 1.909$ Å) at the Institut Laue-Langevin in Grenoble, France. Full patterns (6-158° in 2) were recorded at 300, 200, and 2 K for nuclear and magnetic structure determinations whereas, at intermediate temperatures, partial patterns (6-66° in 2 θ) were utilized for studying the magnetic peaks intensity evolution. Two pattern extracts for each compound are given in figure 1.

At 300 K the observed extinction rules are in agreement with the space groups $F2/m$ and $I2/m$ for $x = 0.25$ and 0.50, respectively. However, for the $x = 0.50$ compound and whatever the temperature, a few weak peaks cannot be indexed but by considering unreacted elemental iron traces. So, the actual composition has to be regarded as slightly lower than 0.50.

As the temperature is lowered below 75 and 130 K for $x = 0.25$ and 0.50, respectively, extra peaks appear. In accord with the magnetic behaviour of these materials as deduced from susceptibility measurements ($T_N = 83$ and 129 K for polycrystalline $x = 0{,}25$ and 0.50 samples, respectively [6], they are attributed to the onset of long range magnetic correlations. With respect to the chemical cells (a, b, c, see the introduction section) and as far as the magnetic cells (am, bm, cm) are concerned, the assignment of the lines leads to :

— a two-fold superstructure for $Fe_{0.25}TiSe_2$ with : $am = a$, $bm = b$ and $cm = 2c$; systematic extinctions for $hm + km + lm = 2n + 1$ ($I2/m$),

— a four-fold superstructure for $Fe_{0.50}TiSe_2$ with : $am = 2a$, $bm = b$ and $cm = 2c$; systematic extinctions for $hm + lm = 2n + 1$ ($B2/m$).

The structure refinements were then carried out according to the Rietveld profile method [8] which enables the minimization of the errors due to overlapping to be done. The computer program allows the atomic occupation rates (Fe/vacancy, Fe/Ti, ...) to be refined with or without constraint. As the scattering lengths of Ti and Fe are markedly different (-0.34 and $+0.95 \times 10^{-12}$ cm for Ti and Fe, respectively), the Bragg peaks intensities are

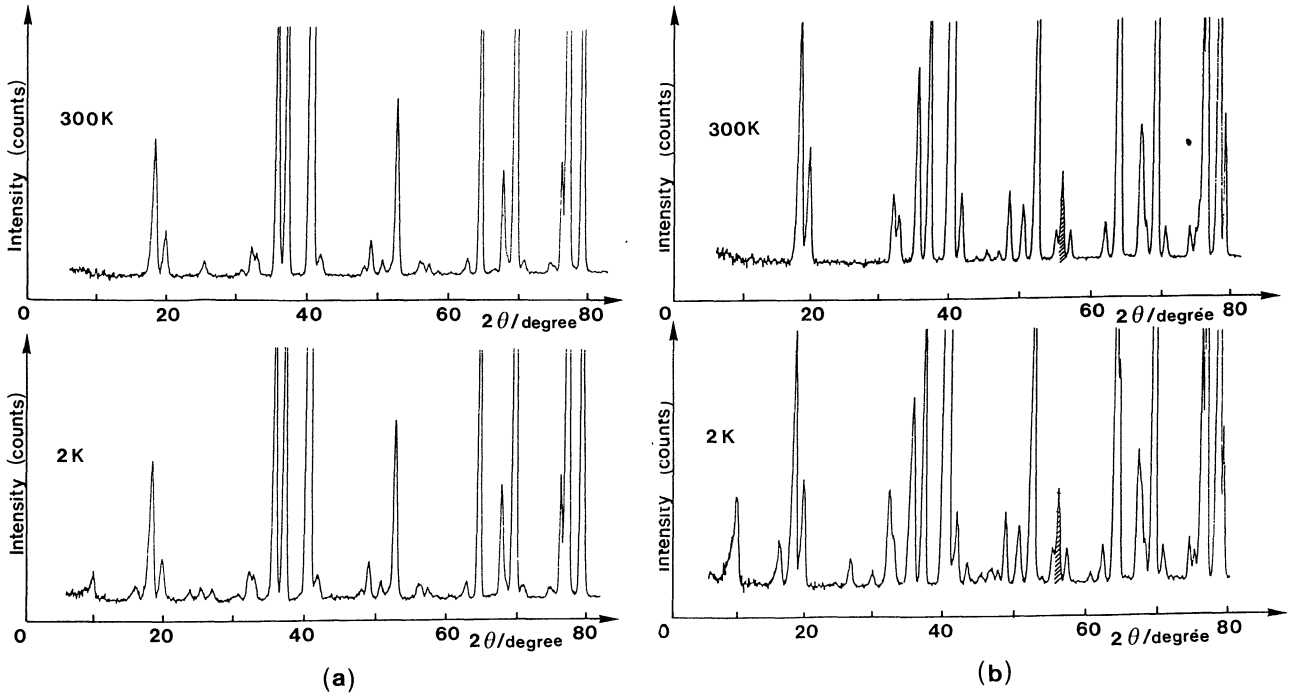

Fig. 1. — Neutron scattering pattern extracts for $Fe_{0.25}TiSe_2$ (a) and $Fe_{0.48}TiSe_2$ (b). The shaded area represents the line due to the presence of a small amount of unreacted iron.

expected to be very sensitive to the Fe-Ti exchanges if any.

3. Crystal structures determination.

3.1 $Fe_{0.48}TiSe_2$. — The room-temperature data refinements were made on the basis of a M_3X_4-type structure ($I2/m$, $Z = 4$). Although the resulting R factor is satisfactory ($R = 0.057$ for 186 used Bragg peaks), significant discrepancies occur between the calculated and observed intensities of a few intense Bragg peaks (e.g. $(I_{obs} - I_{calc})/I_{obs} = 18\,\%$ and 22 % for the 002 and the 101 lines, respectively). In addition, the isotropic thermal parameters of Fe and Ti are large (1.62 and 0.98 Å^2, respectively).

Consequently, several cation-vacancy disorder models were then tested. They turned out to be unvalid. In contrast, taking into account Fe-Ti exchange led to a better fit of the 002 and 101 line intensities (3 and 4 %, respectively). Finally the iron content (x) was refined. But, in order to avoid correlation effects, the calculations were conducted assigning discrete values of x in the range 0.40 – 0.50. For each value, the atomic occupation rates (τ) were refined. The best fit to the data (Tab. I) is obtained for $x = 0.48$, which means that

Table I. — *Unit-cell dimensions and atomic parameters for* $Fe_{0.48}TiSe_2$ *(space group* $I2/m$, $Z = 4$*). Standard deviations in units of the last decimal place are given in parentheses. The* τ_{Ti}*'s are the numbers of titanium atoms per* $Fe_{0.48}TiSe_2$ *formula in the « Fe-layer » and in the « Ti-layer ». The significance of* τ_{Fe} *is similar.*

	$T = 300$ K				$T = 200$ K				$T = 2$ K (Chemical cell)			
a (Å)	6.2673(1)				6.2571(1)				6.2492(1)			
b (Å)	3.5915(1)				3.5846(1)				3.5731(1)			
c (Å)	11.9557(2)				11.9369(2)				11.9324(2)			
β (°)	89.631 (1)				89.623 (1)				89.584 (1)			
	x	y	z	B (Å^2)	x	y	z	B (Å^2)	x	y	z	B (Å^2)
Fe (2/m)	0	0	0	0.78(5)	0	0	0	0.50(4)	0	0	0	0.19(3)
Ti (m)	0.0195(8)	0	0.2504(3)	0.29(7)	0.0174(7)	0	0.2506(3)	0.17(6)	0.0153(7)	0	0.2504(3)	0.02(6)
Se1 (m)	0.1682(3)	1/2	−0.1277(2)	0.61(2)	0.1685(2)	1/2	−0.1273(1)	0.38(2)	0.1685(2)	1/2	−0.1275(1)	0.15(2)
Se2 (m)	0.3392(3)	0	0.1162(1)		0.3391(2)	0	0.1161(1)		0.3389(2)	0	0.1160(1)	
	Fe-layer		Ti-layer		Fe-layer		Ti-layer		Fe-layer		Ti-layer	
τ_{Ti}	0.039(2)		0.961(2)		0.040(2)		0.960(2)		0.039(2)		0.961(2)	
τ_{Fe}	0.441(2)		0.039(2)		0.440(2)		0.040(2)		0.441(2)		0.039(2)	
R (Å)	4.10				3.99				4.29			

0.02 vacancy is randomly distributed over the Fe-site. The R factor then drops to 0.041. From table I, it may be seen that in a « Ti-layer » about 4 % of the sites are actually occupied by Fe atoms, i.e. in a « Fe-layer » about 8 % of the metal sites are occupied by Ti atoms.

The effect of temperature is also shown in table I. Below T_N, no significant change of the non magnetic peak intensities is detected so that the magnetic ordering does not significantly affect the crystal cell symmetry in agreement with the good fit obtained at 2 K (Tab. I).

3.2 $Fe_{0.25}TiSe_2$. — Similarly, the collected data could not be satisfactorily reproduced assuming the ideal Fe and Ti distribution which corresponds to the M_5X_8-type structure, namely iron an Ti segregated in neighbouring planes. Effectively, the R factor is lowered by considering Fe-Ti exchange and the best result is obtained with 2 % of the Ti atoms replaced by Fe atoms in the « Ti-layers », i.e. with 8 % of the Fe atoms replaced by Ti atoms in the « Fe-layers » (Tab. II).

4. Magnetic structures determination.

Figure 2 illustrates the schematic representation of the $x = 0.25$ and 0.48 magnetic structures derived by combining the supercell features as revealed from the 2 K neutron diffraction patterns and the easy-axis direction, perpendicular to the layers, as deduced from the susceptibility measurements [5, 6]. The iron moments at 1/2, 0, 1/4 and 1/4, 1/2, 1/4 (with respect to the magnetic cells), for $x = 0.25$ and 0.48, respectively, have been chosen arbitrarily upwards. Effectively, since the hkl and $\bar{h}kl$ reflections are not resolved ($\beta \simeq 90°$), it is not possible to decide which one of the two possible orientations is

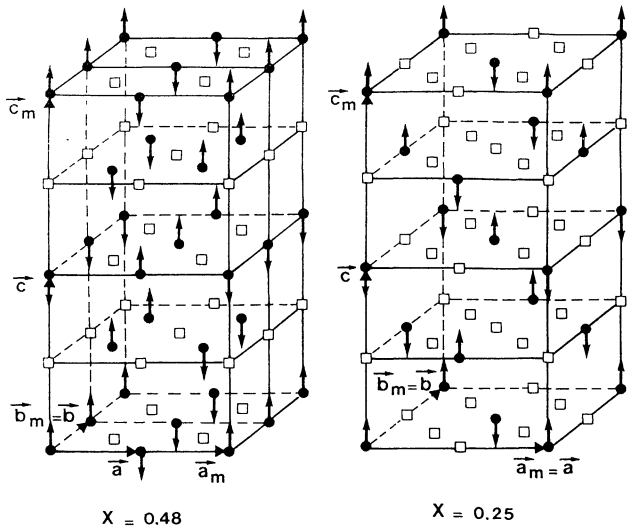

Fig. 2. — Schematic perspective view of the $Fe_{0.48}TiSe_2$ and $Fe_{0.25}TiSe_2$ magnetic structures. Only iron atoms (•) and vacancies (□) are represented.

the actual one. For the purpose of comparison between the two compounds, two magnetic cells have been represented in the b-direction for $x = 0.48$.

For this latter compound, the magnetic structure is of the AF2 type. Respective to the chemical cell, all the spins in the same $(\bar{1}01)$ plane are parallel, and opposite to the spins on the neighbouring $(\bar{1}01)$ plane. As for the $x = 0.25$ material, the spin arrangement may be described as forming two series of antiferromagnetically coupled « ferromagnetic » planes : $(\bar{1}01)$ and (101), with respect to the magnetic cell.

At 2 K, assuming first that Fe alone bears a magnetic moment, the magnetic R factors are 0.23

Table II. — *As table I but for* $Fe_{0.25}TiSe_2$ *(space group* $F2/m$, $Z = 16$*).* τ_{Ti} *and* τ_{Fe} *are given per* $Fe_{0.25}TiSe_2$ *formula.*

	T = 300 K				T = 2 K (Chemical cell)			
a (Å)	12.3628(2)				12.3229(2)			
b (Å)	7.1540(1)				7.1325(1)			
c (Å)	11.9473(2)				11.8939(3)			
β (°)	89.669 (1)				89.669 (1)			
	x	y	z	B (Å²)	x	y	z	B (Å²)
Fe (2/m)	0	0	0	0.61(7)	0	0	0	0.18(6)
Ti1 (m)	0.0039(7)	0	0.2502(5)	0.52(6)	0.0041(6)	0	0.2496(4)	0.04(5)
Ti2 (2)	1/4	0.2414(16)	1/4		1/4	0.2408(14)	1/4	
Se1 (1)	0.0846(6)	0.2533(3)	0.1211(2)	0.51(2)	0.0844(2)	0.2534(3)	0.1207(1)	0.03(2)
Se2 (m)	0.1680(3)	0	−0.1250(2)		0.1680(3)	0	−0.1246(2)	
Se3 (m)	0.3349(3)	0	0.1189(2)		0.3351(2)	0	0.1185(2)	
	Fe-layer		Ti-layer		Fe-layer		Ti-layer	
τ_{Ti}	0.023(1)		0.977(1)		0.022(1)		0.978(1)	
τ_{Fe}	0.227(1)		0.023(1)		0.228(1)		0.022(1)	
R (%)	3.80				3.57			

and 0.34 and the refined Fe(II) magnetic moments values are 4.03(9) and 3.05(5) μ_B for $x = 0.25$ and 0.48, respectively. Owing to the weakness of the $x = 0.25$ magnetic Bragg peaks, the value $R = 0.23$ can be considered as satisfactory. As for the $x = 0.48$ compound, the magnetic Bragg peaks are twice larger on an average so that the value $R_m = 0.34$ indicates a significant misfit. In particular, a somewhat important disagreement is observed between the calculated and observed intensities of the first two main Bragg peaks. All the subsidiary refinements carried out by adding a component of the moment in the layers or considering more complicated arrangements did not lead to any significanty improvement. At higher temperatures (40, 80, 120, and 130 K), the model was similarily found to be inadequate.

Then, for $x = 0.48$, a statistical localized magnetic moment was assigned to every cation of the « Ti-layer ». Several spin arrangements have been checked. Only one (illustrated in Fig. 3) has been found to considerably improve the fit ($R = 0.20$). The refined Ti-Fe magnetic moment value is found rather large (0.43 μ_B). Indeed, assuming the same moment value for Fe in the « Ti-layers » as in the « Fe-layers », and considering the Ti substitution rate refined above, we calculate 0.31 μ_B per atom Ti in the « Ti-layers ». Figure 4 shows the thermal behaviour of the moment assigned to Fe in the « Fe-layers » as well as to Ti in the « Ti-layers ». It may be noticed that both moments vanish at B_N. Besides, we may notice that the Fe moment value is found significantly higher in this second assumption than in the first one (3.38 and 3.05 μ_B, respectively).

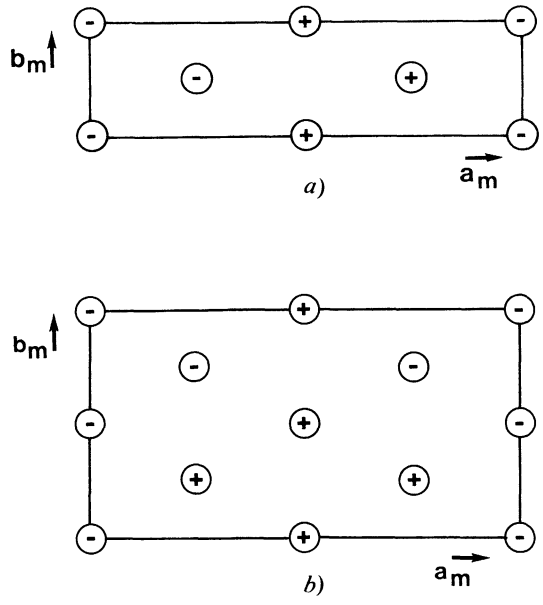

Fig. 3. — Distribution of the Ti magnetic moments in the (001) planes of (a) $Fe_{0.48}TiSe_2$ and (b) $Fe_{0.25}TiSe_2$ (e.g., $z = 1/8$).

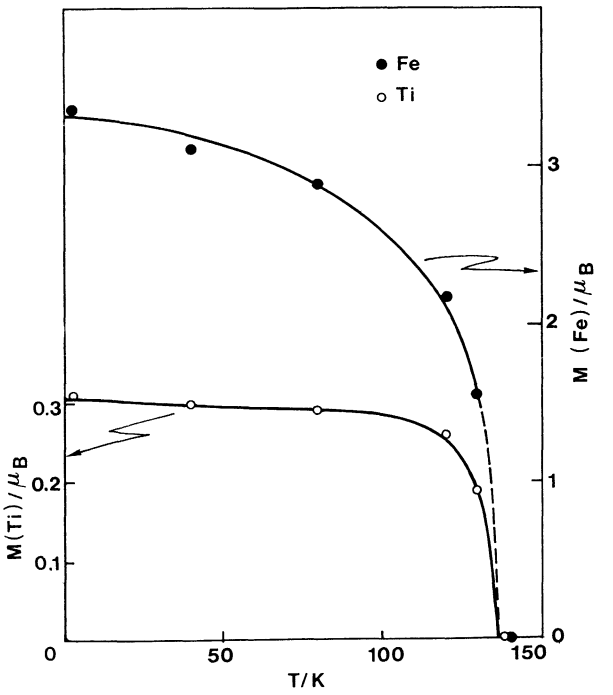

Fig. 4. — Thermal evolution of the magnetic moments of Fe in the « Fe-layer » and Ti in the « Ti-layer » for $Fe_{0.48}TiSe_2$.

Similarly, for $Fe_{0.25}TiSe_2$, taking into account a magnetic moment for Ti as shown in figure 3 improves the fit of the data. Table III gathers all the 2 K refined moment values according to the two above hypotheses. In spite of the large calculated Ti-moment values, the assumption of magnetic Ti-layers is considered as satisfactory since (i) the lowering of the R-factor is appreciable, (ii) the obtained moment value for Fe is closer to the expected spin-only value (4 μ_B) when $x = 0.48$, and (iii) the standard deviations are small, especially for $x = 0.48$.

Table III. — 2 K *moment values* (μ_B) *of* Fe *and* Ti *according to the two hypotheses discussed in the text.*

	Non-magnetic « Ti-layers »		Magnetic « Ti-layers »		
Compound	M (Fe)	R	M (Fe)	M (Ti)	R
$x = 0.25$	4.03(9)	0.23	4.17(9)	0.07(3)	0.19
$x = 0.48$	3.05(5)	0.34	3.38(5)	0.31(3)	0.20

5. Discussion.

5.1 CRYSTAL STRUCTURES ABOVE AND BELOW T_N. — Despite a slight discrepancy from the stoichiometry for as grown $Fe_{0.50}TiSe_2$ (the refined formula is actually $Fe_{0.48}TiSe_2$), the metal-vacancy distribution in the van der Waals gap of the dis-

elenide is found perfectly ordered for both intercalation compounds. Besides, a significant Ti-Fe exchange is observed. Whatever the iron content is, Ti is substituted for 8 % of Fe in the « Fe-layers ». As a result, these compounds cannot be considered as pure intercalation compounds. Such an exchange results from the fact that the studied materials are prepared from the elements at high temperature (800 °C) in contrast with genuine intercalation compounds, e.g. Li_xTiS_2.

Tables IV and V gather the main interatomic distances encountered in the studied compounds as a function of temperature. The average metal-selenide distances are also reported. From these latter values, it may be seen that the Fe- and Ti-containing octahedra are almost of the same size.

However, they can be distinguished by taking into account their respective distortion. Considering a given octahedron, let L be the average Se-Se distance in the layer and H the distance between the centres of the two triangular faces belonging to adjacent layers. The calculated ratios H/L for the two kinds of octahedra in the studied compounds are given in tables VI and VII. Given that for an undistorted octahedron $H/L = \sqrt{2/3} = 0.817$, we find that the $[FeSe_6]$ octahedron is on average not distorted along the direction perpendicular to the layers, within the experimental accuracy. In contrast, the $[TiSe_6]$ octahedron is elongated.

Table IV. — *Main interatomic distances* (Å) *in* $Fe_{0.25}TiSe_2$ *at several temperatures. The standard deviations are independent of temperature.*

Bond and multiplicity		300 K d (Å)	300 K average	2 K d (Å)	2 K average
$Fe\text{-}Se_1$	(× 4)	2.547(3)	2.548	2.535	2.536
$Fe\text{-}Se_2$	(× 2)	2.551(4)		2.539	
$Ti_1\text{-}Se_1$	(× 2)	2.577(9)	2.577	2.565	2.569
$Ti_1\text{-}Se_{1'}$	(× 2)	2.580(9)		2.577	
$Ti_1\text{-}Se_2$	(× 1)	2.606(13)		2.597	
$Ti_1\text{-}Se_3$	(× 1)	2.540(11)		2.534	
$Ti_2\text{-}Se_1$	(× 2)	2.568(3)	2.567	2.564	2.562
$Ti_2\text{-}Se_2$	(× 2)	2.581(10)		2.578	
$Ti_2\text{-}Se_3$	(× 2)	2.553(9)		2.545	

Table V. — *As table IV but for* $Fe_{0.48}TiSe_2$.

Bond and multiplicity		300 K d (Å)	300 K average	200 K d (Å)	200 K average	2 K d (Å)	2 K average
$Fe\text{-}Se_1$	(× 4)	2.578(1)	2.568	2.571	2.561	2.567	2.557
$Fe\text{-}Se_2$	(× 2)	2.547(1)		2.542		2.538	
$Ti\text{-}Se_1$	(× 2)	2.603(7)	2.587	2.599	2.584	2.586	2.580
$Ti\text{-}Se_{1'}$	(× 1)	2.634(7)		2.617		2.603	
$Ti\text{-}Se_2$	(× 1)	2.557(7)		2.566		2.572	
$Ti\text{-}Se_{2'}$	(× 2)	2.563(7)		2.563		2.566	

Table VI. — *Distortion of the* Fe- *and* Ti-*containing octahedra as a function of temperature for* $Fe_{0.48}TiSe_2$. *The H/L ratio is defined in section* 5.1.

T (K)	H/L (Fe)	H/L (Ti)
300	0.815(2)	0.849(2)
200	0.813(2)	0.851(2)
T_N		
2	0.816(2)	0.852(2)

Table VII. — *As table VI, but for* $Fe_{0.25}TiSe_2$.

T (K)	H/L (Fe)	H/L (Ti_1)	H/L (Ti_2)
300	0.809(2)	0.858(2)	0.860(2)
T_N			
2	0.805(2)	0.860(2)	0.861(2)

Furthermore, the elongation of the $[TiSe_6]$ octahedron decreases as x increases. This change may be interpreted in terms of the Jahn-Teller effect, as follows. As the iron content is increased, the number of donated electrons from Fe to $TiSe_2$ increases according to :

$$x\mathrm{Fe} + \mathrm{TiSe_2} \rightarrow \mathrm{Fe}_x^{II}\,\mathrm{Ti}_{2x}^{III}\,\mathrm{Ti}_{(1-2x)}^{IV}\,\mathrm{Se_2}\,,$$

leading to a dz^2 band which is 1/4 filled for $Fe_{0.25}TiSe_2$ and 1/2 filled for $Fe_{0.48}TiSe_2$, the z-axis being perpendicular to the layers [9]. The H/L ratio decrease from $x = 0.25$ to $x = 0.48$ hence arises from the fact that the energy lowering needs less distortion as the band filling increases.

For $x = 0.48$, from the existence of magneto-elastic effects [6], it could be expected that an abrupt change in the H/L ratio should occur at T_N for the Fe-containing octahedron. However the experimental accuracy is not sufficient for the calculated H/L evolution (Tab. VI) to be really significant.

5.2 MAGNETIC STRUCTURES. — Figure 5 illustrates the magnetic structures of both compounds in the « Fe-layers ».

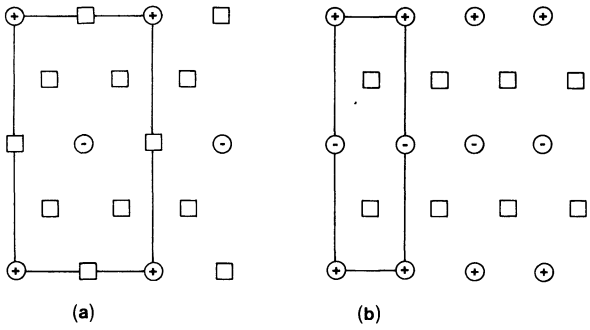

Fig. 5. — Distribution of the Fe magnetic moments in the (001) planes of $Fe_{0.25}TiSe_2$ (a) and $Fe_{0.48}TiSe_2$ (b). (+) is for spin up and (−) is for spin down. The solid lines represent the magnetic cells.

For $x = 0.25$, the magnetic sublattice which is in the (001) planes is triangular. The nearest neighbouring (n.n.) interacting iron ions are separated by a distance equal to 7.1 Å. The magnetic structure may hence be interpreted as resulting from the existence of antiferromagnetic n.n. interactions. Given that the magnetic sublattice is triangular and that the susceptibility curves are consistent with an Ising model [5, 6], the AF character of the interactions should lead to frustration effects and, consequently, to a paramagnetic behaviour down to 0 K [10]. The transition below 83 K is thus to be attributed to the influence of interlayer interactions which couple the frustrated planes together.

On the other hand, it is worthy of note that such an assumed frustration in the layers could be at the origin of the spin-glass behaviour of the disorderly diluted compounds with lower iron contents ($x < 0.20$) which has been observed by Huntley *et al.* [4]. This latter argument holds provided that the $x = 0.25$ lattice overall geometry is unchanged as x diminishes. It could also apply to the related Fe_xZrX_2 ($x < 0.25$) spin glasses [11]. However, as far as the titanium compounds ($x < 0.20$) are concerned, the RKKY coupling between the iron moments *via* the conduction electrons in the adjacent layers are likely to contribute also to the origin of the magnetic behaviour.

For $x = 0.48$, the magnetic sublattice in one layer derives from the observed one for $x = 0.25$ by filling the vacancies along the b-axis. « Ferromagnetic » chains result from such an arrangement (Figs. 2 and 5), in accord with the predicted predominantly F character of the n.n. interactions (see the introduction section). From one chain to the next, the magnetic pathway along the (110) direction (with respect to the chemical cell) is the same as the n.n. pathway for $x = 0.25$ (Fig. 5) which is AF as discussed above. An AF coupling of the chains is thus expected in agreement with the observed AF structure.

Finally, the most interesting result of the study is the occurrence below T_N of a large moment borne by the Ti ions in the metallic [12] « Ti-layers » for both compounds (Tab. III). The existence of a calculated Ti partial moment is to be attributed to the interaction of the Ti conduction electrons with the localized Fe moments as previously discussed [6]. This is consistent with the analysis by Antoniou [13] concerning iron-doped $TaSe_2$, which is based on the formation of a spin-density wave state (SDW) [14] and also with the work by Parkin *et al.* as regards $Mn_{0.25}TaS_2$ [15] in which they have shown through a neutron diffraction study that about 15 % of the Mn moments are lost for the benefit of Ta. The periodicity of the spin density in the « Ti-layers » is the same as in the « Fe-layers » (Figs. 3 and 5). We also note that the Ti polarized moment value for $x = 0.48$ is equal to about four times the value for $x = 0.25$ instead of about twice as predicted on the ground of the respective iron contents. Since in addition the interaction between localized and delocalized electrons is smaller for $x = 0.48$ [6], we deduce that, for this compound, the SDW state stability is enhanced.

Acknowledgments.

The authors express their gratitude to Dr. Hewat for his help in carrying out the neutron diffraction experiments.

References

[1] YOFFE, A. D., *Physics and chemistry of Electrons and Ions in Condensed Matter,* J. V. Acrivos, N. F. Mott and A. D. Yoffe (eds), NATO ASI Series (D. Reidel Publishing Company) 1984, p. 437 ;
BEAL, A. R., *Intercalated Layered Materials,* F. A. Lévy, ed. (D. Reidel Publishing Company) 1979, p. 251.

[2] ARNAUD, Y., CHEVRETON, M., AHOUANDJINOU, A., DANOT, M. and ROUXEL, J., *J. Solid State Chem.* **18** (1976) 9.

[3] CHEVRETON, M., *Bull. Soc. Fr. Minéral. Cristallogr.* **XC** (1967) 592.

[4] HUNTLEY, D. R., STENKO, M. J. and HIEBL, K., *J. Solid State Chem.* **52** (1984) 233.

[5] MURANAKA, S. and TAKADA, T., *J. Solid State Chem.* **14** (1975) 291.

[6] BUHANNIC, M. A., COLOMBET, P., DANOT, M. and CALVARIN, G., *J. Solid State Chem.* **69** (1987).

[7] FATSEAS, G. A., DORMANN, J. L. and DANOT, M., *J. Physique Colloq.* **40** (1979) C2-367.

[8] RIETVELD, H. M., *J. Appl. Crystallogr.* **2** (1969) 65 ;
HEWAT, A. W., Harwell Report, AERE-R7350 (1973).

[9] LIANG, W. Y., *Physics and Chemistry of Electrons and Ions in Condensed Matter,* J. V. Acrivos, N. F. Mott and A. D. Yoffe (eds), NATO ASI series (D. Reidel Publishing Company) 1984, p. 459.

[10] GREST, G. S. and GABL, E. G., *Phys. Rev. Lett.* **43** (1979) 1182.

[11] BUHANNIC, M. A., DANOT, M. and COLOMBET, P., *Nouv. J. Chim.* **9** (1985) 405 ;
BUHANNIC, M. A., COLOMBET, P. and DANOT, M., *Solid State Commun.* **59** (1986) 77 ;
BUHANNIC, M. A., DANOT, M., COLOMBET, P., DORDOR, P. and FILLION, G., *Phys. Rev.* **B 34** (1986) 4790.

[12] AHOUANDJINOU, A., *Thesis,* University of Nantes, France (1977).

[13] ANTONIOU, P. D., *Phys. Rev.* **B 20** (1979) 231.

[14] ARROTT, A., *Magnetism,* G. T. Rado and H. Suhl (eds) (Academic Press) Vol. II B (1966) 295.

[15] PARKIN, S. S. P., MARSEGLIA, E. A. and BROWN, P. J., *J. Phys.* **C 16** (1983) 2769.